Glassy Statics and Dynamics in the Chemically Ordered Pyrochlore Antiferromagnet $Y_2Mo_2O_7$

J. S. Gardner,[1] B. D. Gaulin,[1] S.-H. Lee,[2] C. Broholm,[2,3] N. P. Raju,[4] and J. E. Greedan[4]
[1]*Department of Physics and Astronomy, McMaster University, Hamilton, Ontario, Canada L8S 4M1*
[2]*National Institute of Standards and Technology, Gaithersburg, Maryland 20899*
[3]*Department of Physics and Astronomy, The John Hopkins University, Baltimore, Maryland 21218*
[4]*Brockhouse Institute for Materials Research, McMaster University, Hamilton, Ontario, Canada L8S 4M1*
(Received 4 January 1999)

Static and dynamic magnetic correlations in the geometrically frustrated pyrochlore antiferromagnet $Y_2Mo_2O_7$ have been studied using neutron scattering. The material is chemically ordered but displays a spin-freezing transition at $T_g \sim 22.5$ K. We show that dynamic short range order develops below room temperature. Upon cooling the two-spin correlation length never exceeds 5 Å, yet the spin fluctuation rate vanishes in proportion to $T - T_g$. For $T < T_g$ low energy spin fluctuations are replaced by static antiferromagnetic short range order with a frozen staggered magnetization $|\langle \mathbf{S} \rangle|/S \approx 0.67(2)$. Locally the frozen spin structure corresponds to four sublattice ordering with zero magnetization.

PACS numbers: 75.50.Lk, 75.25.+z, 75.40.Cx, 75.40.Gb

Materials which possess the combination of antiferromagnetism and lattice symmetries based on triangles and tetrahedra have the potential to display phenomena known as *geometrical frustration* [1]. These local symmetries disfavor two sublattice Néel ordering, as it is impossible to satisfy all near neighbor antiferromagnetic (AFM) couplings, and an intrinsic competition exists between ground states favored by different pairs of neighbors. Competing interactions have motivated much current activity in physics, but this has mainly focused on phenomena wherein the competition arises due to the combination of long range interactions and chemical disorder, as is the case in conventional spin glasses [2].

The oxide pyrochlore family, with composition $A_2B_2O_7$, crystallizes into a face centered cubic structure [3]. The *A* site which has eightfold oxygen coordination is occupied by a trivalent rare earth ion, while the sixfold coordinated *B* site is occupied by a tetravalent transition metal ion. The *A* and *B* sites form interpenetrating sublattices of corner-sharing tetrahedra. If either of these sites is magnetic with a dominant AFM nearest neighbor interaction, then a high degree of frustration and a potential for unusual magnetic behavior exists.

One characteristic of many of the geometrically frustrated pyrochlores is that they show classic spin-glass behavior in bulk magnetic properties. These effects include both history dependencies and divergent nonlinearities in their magnetic susceptibilities. This behavior has been extensively studied in $Y_2Mo_2O_7$ [4], but has also been observed in other oxide pyrochlores, such as $Tb_2Mo_2O_7$ [5] and $Y_2Mn_2O_7$ [6], as well as the disordered pyrochlore $CsNiCrF_6$ [7] and the disordered two dimensional kagomé-like system $SrCr_{9p}Ga_{12-9p}O_{19}$ (SCGO) [8,9]. It is unexpected in the oxide pyrochlores as it is generally accepted that a spin glass results from the combination of frustration and either site or bond disorder, while all diffraction studies of the oxide pyrochlores have found them to be periodic solids [10]. It is therefore important to understand the nature of the magnetic ground state of $Y_2Mo_2O_7$, and to establish its relation to the low temperature state of conventional spin glasses.

Theoretically, such systems have received much attention beginning with Anderson's classic treatment in 1956 [11]. Recently, it has been shown that near neighbor Heisenberg AFM interactions between either classical [12] or quantum spin-$\frac{1}{2}$ moments [13] on a pyrochlore lattice should display only local order on individual tetrahedra. It has been suggested that nonergodic spin-glass-like states may occur for some frustrated magnets without quenched disorder [14,15]; however, Moessner and Chalker [12] have shown that this should not occur for the *classical* pyrochlore AFM.

$Y_2Mo_2O_7$ is a narrow band semiconductor with a cubic lattice parameter $a = 10.21$ Å at 4 K. A Curie-Weiss fit to the high temperature (300–1000 K) susceptibility yields $\Theta_{CW} \sim -200$ K [16], indicating strong AFM interactions and an effective moment of $2.55\mu_B$ close to the effective moment $g\sqrt{S(S+1)}\,\mu_B = 2.8\mu_B$ expected for $S = 1$ Mo^{4+}. Low field magnetization versus T shows a cusp at $T_g = 22.5$ K with strong irreversibilities below T_g as in chemically disordered spin glasses, such as CuMn, EuSrS, and CdMnTe [2]. In this Letter, we report detailed neutron scattering studies of $Y_2Mo_2O_7$ that directly reveal the static and dynamic magnetic correlations underlying the spin-glass-like properties of this chemically ordered compound.

The 40 g polycrystalline sample of $Y_2Mo_2O_7$ used in these studies was prepared by firing, at 1350 °C, stoichiometric amounts of Y_2O_3 and MoO_2 for several days in an argon atmosphere with intermittent grindings to ensure complete reaction. Field-cooled and zero field-cooled magnetization measurements were performed to determine T_g and these data were indistinguishable from that reported previously [4]. We established the crystal structure of our sample by neutron powder diffraction on

the BT1 diffractometer at the National Institute of Standards and Technology (NIST). The structural parameters, extracted using Rietveld refinement, were consistent with previous work [10]. The data place an upper limit of 4% on *A-B* site mixing and 1% on deviations from nominal oxygen stoichiometry in our sample.

For inelastic scattering we used the SPINS triple axis spectrometer at NIST. Cold neutrons reach the instrument through an evacuated ^{58}Ni coated rectangular guide. A vertically focusing pyrolytic graphite (PG) (002) monochromator focuses $(6–8.5) \times 10^6$ neutrons $\mathrm{cm}^{-2}\,\mathrm{s}^{-1}$ onto the sample for $3.7 < E_i < 7$ meV. Scattered neutrons are analyzed with eleven 2.1 cm $\times$ 15 cm cylindrical ^{3}He proportional counter located 36 cm from the center of the analyzer. For measurements requiring good Q resolution, we used three parallel analyzer blades and a 40′ collimator after the sample. For measurements with coarse Q resolution, 5-11 blades were arranged to reflect neutrons monochromatically onto the detector. We used fixed final energies of $E_f = 3.7$ and $E_f = 5.1$ meV yielding elastic energy resolutions of 0.12 and 0.28 meV, respectively. Cooled Be and BeO filters were used to suppress higher order contamination and background. All data were normalized as described in Ref. [17].

Elastic scattering measurements, using $E_f = 5.1$ meV and a flat analyzer, were performed at 1.8 and 50 K. The difference between the two data sets shown in Fig. 1 is a measure of the low temperature elastic magnetic structure factor $\overline{S}(Q)$. The data show a peak for $Q \approx 0.44$ Å^{-1}, indicating short range AFM correlations on a time scale $\tau > \hbar/\Delta E = 3$ ps. From the half width at half maximum (HWHM) we extract a correlation length $\xi \approx 1/\mathrm{HWHM} \approx 5$ Å, implying correlated domains

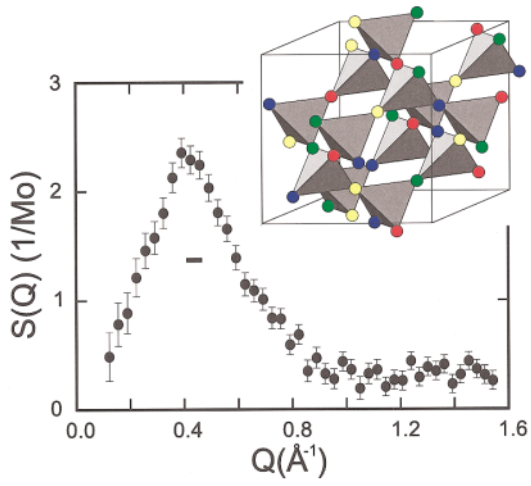

FIG. 1(color). The Q dependence of elastic magnetic scattering in $Y_2Mo_2O_7$ at $T = 1.4$ K. Data taken at 50 K have been subtracted to account for the nuclear scattering. Inset: A four sublattice spin arrangement for short range order in $Y_2Mo_2O_7$ that is consistent with the periodicity derived from the diffraction.

extending over a single conventional unit cell. The short range AFM order in $Y_2Mo_2O_7$ is a longer wavelength local structure than in $Tb_2Ti_2O_7$ [18], where Tb spins are correlated over a single tetrahedron only. In fact, $Tb_2Ti_2O_7$ displays no phase transitions of any kind, remaining a "cooperative paramagnet" down to at least 70 mK. The position of the first peak in the diffuse magnetic scattering from $Tb_2Ti_2O_7$ [18] is $\sim$1.2 Å^{-1}, close to $4\pi/d(001)$, where $d(001) \sim 10.2$ Å, and this implies AFM correlations between pairs of spins making up a single tetrahedron. For $Y_2Mo_2O_7$, the peak in the diffusion scattering occurs for $Q \approx 2\pi/d(110)$, where $d(110) \approx \sqrt{2} \times 10.2$ Å is the diagonal of a cube face. Such a local periodicity permits a four sublattice structure along [110] which is displayed schematically in the inset of Fig. 1. Each of the four sublattices is indicated by a different color, and the $\Sigma_i \mathbf{S}_i = 0$ constraint over a single tetrahedra which is implied by the vanishing of elastic scattering for $Qa \rightarrow 0$ can be fulfilled by requiring that each tetrahedra be color neutral. This local structure is the tetrahedral analog of that exhibited in SCGO [8,9], where a three sublattice local structure is relevant, as that structure is based on triangles. It also implies a large ground state degeneracy within the pyrochlore structure as neighboring chains along perpendicular [110] directions share only a single tetrahedron. The magnitude of the frozen staggered magnetization is derived by integrating the elastic scattering data: $|M|^2 \approx (3/2) \int_{0.16\ \text{Å}^{-1}}^{1\ \text{Å}^{-1}} Q^2\,dQ \times [\overline{S}(Q)/|F(Q)|^2] / \int Q^2\,dQ \approx 1.80(8)$. Assuming that $g \approx 2$ this implies that $|\langle \mathbf{S} \rangle|/S \approx 0.67$ which is an unusually small number for a three dimensional magnet in the limit $T/\Theta_{\mathrm{CW}} \rightarrow 0$. The temperature dependence of the elastic diffuse scattering at $Q = 0.44$ Å^{-1} is shown in Fig. 2(a). The nominally elastic scattering within the $\Delta E = 0.2$ meV energy window of the spectrometer is only weakly temperature dependent above 50 K, but shows a very pronounced increased below 40 K. The glass temperature T_g lies roughly in the middle of the regime which displays strong growth with decreasing T.

Inelastic neutron scattering measurements for Q near the maximum in the diffuse scattering were performed at temperatures of 1.5 K and above using the horizontally focusing analyzer. Because inelastic magnetic scattering from $Y_2Mo_2O_7$ is strongly suppressed below T_g, the $T = 1.5$ K data set was an excellent measure of the background for $|\hbar\omega| < 2.5$ meV. An overview of these data is shown in a color contour map of $S(Q, \omega)$ vs $\hbar\omega$ and T in Fig. 3(a). Several features are striking on examination of the data. Low energy spin fluctuations develop below 45 K and progressively sharpen in frequency on lowering temperature. The glass temperature T_g manifests itself as the temperature where the low frequency scattering collapses into the elastic peak. Consequently, there are three temperature regimes for $S(Q, \omega)$. For $T > 55$ K, $S(Q, \omega)$ displays a rather broad frequency spectrum. For $T_g < T < 50$ K, the inelastic scattering

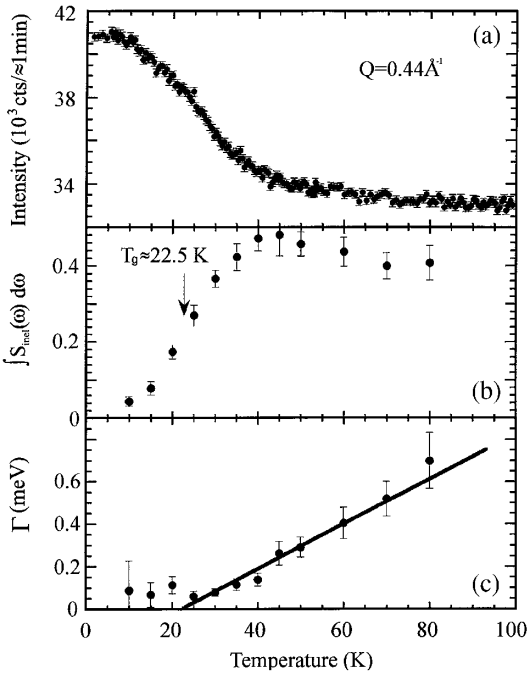

FIG. 2. (a) Temperature dependence of elastic scattering at the peak in the structure factor, $Q = 0.44$ Å^{-1}. (b) Temperature dependence of the energy integral of $S(Q, \omega)$ which is a measure of the squared amplitude of spin fluctuations. (c) Temperature dependence of the characteristic relaxation rate Γ derived from the fits shown in Fig. 3(b).

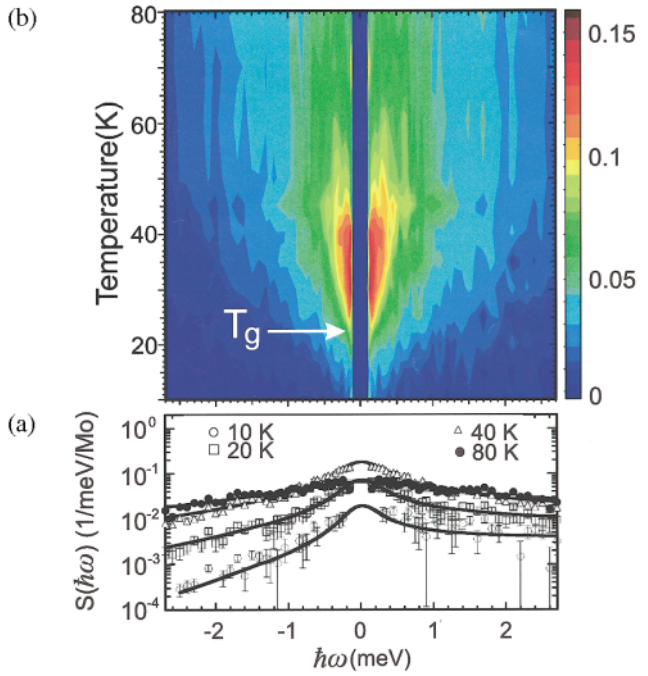

FIG. 3(color). (a) Background-subtracted and normalized inelastic scattering data for $S(Q, \omega)$ at twelve temperatures between 10 and 80 K. (b) Representative energy scans from which the color contour map was made, along with fits to the data as described in the text.

is greatly enhanced at low frequencies in what resembles a critical regime, and finally this inelastic scattering is strongly suppressed below T_g as the elastic scattering associated with the spin-glass order parameter develops. A quantitative analysis of the inelastic scattering was also carried out. The data were fit to an appropriate resolution convolution of

$$S(\hbar\omega) = \frac{1}{\pi}\chi''(\hbar\omega)[1 + n(\hbar\omega)], \qquad (1)$$

where $n(\hbar\omega)$ is the Bose thermal population factor, and the imaginary part of the dynamic susceptibility is given by

$$\chi''(\hbar\omega) = \chi_0 \arctan\left(\frac{\omega}{\Gamma}\right). \qquad (2)$$

The characteristic relaxation rate Γ corresponds to the low frequency cutoff of an otherwise frequency independent fluctuation spectrum [19]. The comparison of the model and data in Fig. 3(b) shows that these formulas yield a good phenomenological description of the energy scans at all temperatures. The temperature dependence of the relaxation rate Γ is shown in Fig. 2(c), and it displays softening at T_g as for a conventional second order phase transition. Figure 2(b) shows $\hbar \int_{-3\ \mathrm{meV}}^{3\ \mathrm{meV}} S(\hbar\omega)\, d\omega$ which is a measure of the squared amplitude of low energy spin fluctuations. The increase of elastic scattering below T_g mirrors the decrease in the inelastic scattering intensity indicating that no modification of the spectrum beyond 3 meV $\approx k_B T_g$ is required to satisfy the total moment sum rule.

The behavior, near and above T_g, bears some resemblance to that displayed by the two dimensional kagomé-like magnet, SCGO [8] in that the characteristic relaxation rate Γ rises approximately linearly with $(T - T_g)$ above T_g. There are however important differences as well. In SCGO strong fluctuations persist below the freezing temperature, while in $Y_2Mo_2O_7$ the amplitude of low energy fluctuations is strongly suppressed below T_g [see Fig. 2(b)]. Moreover, the fluctuation spectrum for $Y_2Mo_2O_7$ does not seem to evolve for $T < T_g$ but remains featureless for $|\hbar\omega| < 1$ meV, while in SCGO Γ increases to a value of order $k_B T_g$ as T is reduced below T_g. Finally, and perhaps most importantly, spin fluctuations in $Y_2Mo_2O_7$ are classical for $T < 5T_g$ in the sense that $k_B T_g \gg \Gamma$ at all T, while the reverse is true for SCGO except in the immediate vicinity of T_g. Spin dynamics in $Y_2Mo_2O_7$ is also *dissimilar* to observations in isostructural $Tb_2Ti_2O_7$ [18], wherein a gapped excitation spectrum incompletely softens at the wave vector characterizing the very short range magnetic order.

Figure 4 shows $\chi''(Q, \hbar\omega = 0.5\ \mathrm{meV})$ as a function of Q which provides information about short range spatial correlations. At all temperatures probed there is a low Q maximum. The peak becomes more pronounced upon cooling until $T = 40$ K, at which point the Q dependence at $\hbar\omega = 0.5$ meV is indistinguishable from

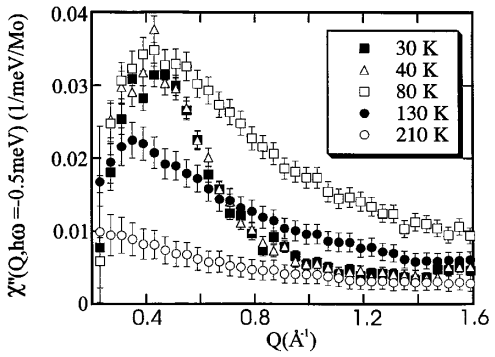

FIG. 4. The Q dependence of $\chi''(Q, \hbar\omega = 0.5$ meV) derived from scattering data via the fluctuation dissipation theorem for $T_g < T < \Theta_{\mathrm{CW}}$. We used $E_f = 3.7$ meV and five focused analyzer blades which yield $\Delta Q = 0.14$ Å^{-1}. Background data at $\hbar\omega = -0.5$ meV and $T = 1.5$ K were subtracted from all data sets.

that associated with static spin correlations at $T = 1.6$ K (Fig. 1). The only change in spin correlations below $T = 40$ K $\approx 2T_g$ therefore seems to be that slow fluctuations are replaced by static correlations as shown in Figs. 2(a) and 2(b).

In summary our experiments show the freezing transition in $Y_2Mo_2O_7$ to be dynamical in nature, occurring almost completely in the frequency domain, and reveals four temperature regimes relevant to the material. At temperatures above $\Theta_{\mathrm{CW}} \sim 200$ K paramagnetic behavior is observed with no significant magnetic correlations in either space or time. Short range correlations develop below 200 K, and these remain broad in energy, but peak up in wave vector around $Q \approx 0.44$ Å^{-1}. For $T_g < T < 2T_g$ there is little or no evolution in spatial correlations, but the characteristic relaxation rate Γ of the "thermal" ($k_B T \gg \hbar\Gamma$) spin fluctuation spectrum decreases in proportion to $T - T_g$ as for critical fluctuations above a second order phase transition to an ordered state. It is within this temperature regime that nonlinearities develop in the susceptibility [4], which head toward a divergence at T_g. This regime is also characterized by a rapid increase of roughly 2 orders of magnitude in the spin relaxation rate $1/T_1$ measured by μSR [20]. Below T_g, low energy spin fluctuations are strongly suppressed, resulting in a concentrated spin-glass-like state with the local four sublattice structure shown in Fig. 1 and sublattice magnetization $|\langle \mathbf{S} \rangle|/S \approx 0.67$.

Short range frozen AFM correlations with little or no quenched disorder, a vanishing spin relaxation rate at T_g, reduced sublattice magnetization, and the local cancellation of magnetization are common features of the strongly geometrically frustrated magnets studied so far. Our experiment on $Y_2Mo_2O_7$ however also shows that there can be significant differences even between isostructural systems, and this highlights the need for theoretical work which takes into account the unique subleading order properties of specific geometrically frustrated model systems.

We thank S. Dunsiger, M. J. P. Gingras, R. F. Kiefl, M. D. Lumsden, R. Moessner, and C. V. Stager for their contributions. This research was funded by NSERC under the Collaborative Research Grant, Geometrically Frustrated Magnetic Materials, and by the NSF under DMR-9453362. We utilized neutron research facilities supported by NIST and the NSF under Agreement No. DMR-9423101.

[1] For recent reviews, see A. P. Ramirez, Annu. Rev. Mater. Sci. **24**, 453 (1994); *Magnetic Systems with Competing Interactions*, edited by H. T. Diep (World Scientific, Singapore, 1994); P. Schiffer and A. P. Ramirez, Comments Condens. Matter Phys. **18**, 21 (1996).
[2] J. A. Mydosh, *Spin Glasses* (Taylor and Francis, London, 1993).
[3] M. A. Subramanian, G. Avravamudan, and G. V. Subba Rao, Prog. Solid State Chem. **15**, 55 (1983).
[4] M. J. P. Gingras *et al.*, Phys. Rev. Lett. **78**, 947 (1997).
[5] B. D. Gaulin *et al.*, Phys. Rev. Lett. **69**, 3244 (1992).
[6] J. N. Reimers *et al.*, Phys. Rev. B **43**, 3387 (1991); Y. Shimakawa *et al.*, Phys. Rev. B **59**, 1249 (1999) report different results.
[7] M. J. Harris *et al.*, Phys. Rev. Lett. **73**, 189 (1994).
[8] S.-H. Lee *et al.*, Europhys. Lett. **35**, 127 (1996).
[9] C. Broholm *et al.*, Phys. Rev. Lett. **65**, 3173 (1990).
[10] J. N. Reimers and J. E. Greedan, J. Solid State Chem. **72**, 390 (1988).
[11] P. W. Anderson, Phys. Rev. **102**, 1008 (1956); see also J. Villain, Z. Phys. B **33**, 31 (1979); J. N. Reimers *et al.*, Phys. Rev. B **43**, 865 (1991); **45**, 7287 (1992); J. T. Chalker *et al.*, Phys. Rev. Lett. **68**, 885 (1992); J. N. Reimers and A. J. Berlinsky, Phys. Rev. B **48**, 9539 (1993).
[12] R. Moessner and J. T. Chalker, Phys. Rev. Lett. **80**, 2929 (1998).
[13] B. Canals and C. Lacroix, Phys. Rev. Lett. **80**, 2933 (1998).
[14] P. Chandra *et al.*, J. Phys. (Paris) I **3**, 591 (1993).
[15] G. Aeppli and P. Chandra, Science **275**, 177 (1997).
[16] N. P. Raju *et al.*, Phys. Rev. B **46**, 5405 (1992).
[17] S.-H. Lee *et al.*, Phys. Rev. B **56**, 8091 (1997).
[18] B. D. Gaulin *et al.*, Physica (Amsterdam) **241B–243B**, 511 (1998); J. S. Gardner *et al.*, Phys. Rev. Lett. **82**, 1012 (1999).
[19] G. Aeppli and T. F. Rosenbaum, in *Dynamical Properties on Unconventional Magnetic Systems*, edited by A. T. Skeltorp and D. Sherrington (Kluwer Academic Press, Dordrecht, The Netherlands, 1998).
[20] S. R. Dunsiger *et al.*, Phys. Rev. B **54**, 9019 (1996).